JOURNAL OF PHYSICAL ORGANIC CHEMISTRY
J. Phys. Org. Chem. 2007; **20:** 297–306
Published online 30 March 2007 in Wiley InterScience
(www.interscience.wiley.com) DOI: 10.1002/poc.1127

Relationship between substituent effect and aromaticity – Part III: naphthalene as a transmitting moiety for substituent effect

Tadeusz M. Krygowski,[1]* Marcin Palusiak,[2] Anna Płonka[1] and Joanna E. Zachara-Horeglad[1]

[1]Department of Chemistry, Warsaw University, Pasteura 1, 02-093 Warsaw, Poland
[2]Department of Crystallography and Crystal Chemistry, University of Łódź, Pomorska 149/153, 90-236 Łódź, Poland

Received 11 August 2006; revised 6 October 2006; accepted 9 October 2006

ABSTRACT: Molecular geometry of 10 isomeric nitronaphtholate ions (excluding *peri*- and *ortho*-type substituted systems), 1- and 2-naphtholate ions, 1- and 2-nitronaphthalene, *meta*- and *para*-nitrophenolate, phenolate, and nitrobenzene were optimized at B3LYP/6-311G** level of approximation. Substituent effect stabilization energy (SESE), geometry-based aromaticity index HOMA, magnetism-based indices NICS, NICS(1), NICS(1)$_{zz}$, and parameters characterizing Bond Critical Points (BCP) (ρ, $\bigtriangledown^2\rho$, ellipticity, ion/cov) of the Bader AIM theory were used to characterize transmitting properties for substituent effect through the naphthalene moiety. It results from our study that the studied systems could be clearly divided into two groups, (i) a *para*-type group, where the intramolecular charge transfer between the π-electron donating and π-electron accepting substituents can be described by canonical forms with charge separation (as in the case of *para*-nitrophenolate) and (ii) a *meta*-type group, where this transfer requires using canonical forms with double charge separation (as in the case of *meta*-nitrophenolate).

KEYWORDS: substituent effect; aromaticity; AIM analysis; naphthalene derivatives; DFT

INTRODUCTION

The influence of substituent on chemical and physicochemical properties of aromatic systems has rich literature.[1] To quantify this effect, a concept of substituent constants, which quantitatively 'measure a change in electron density produced by substituent'[2] has been proposed. For this purpose, *meta*- and *para*-substituted benzoic acids have been chosen as model systems along with appropriate ionization constants as a numerical quantitative characteristic.[3] Even at an early stage of investigations, the problem of some inconsistency in using the originally defined substituent constants for *p*-disubstituted systems appeared,[1b] and new scales of σ_p had to be introduced.[4,5] A modified approach accounted for different electronic mechanism of the substituent effect than that for *meta*- and *para*-substituted benzoic acids. Undoubtedly, interactions between the substituent and the reaction site in benzene (or another substituent attached in *meta* or *para* position) differ substantially as far as the blend of inductive and resonance interactions is concerned. The *meta*-type interactions are mostly inductive/field in nature[6,7] and resonance contribution accounts for only about 30% of the total effect.[8] In the case of *para*-type interactions, the resonance is much stronger. This is nicely illustrated by canonical structures of two typical *p*- and *m*-disubstituted benzene derivatives with π-electron donating (D) and π-electron accepting (A) substituents as shown in Schemes 1 and 2.

For *para*-disubstituted systems apart from canonical forms with charge separation at carbon atoms in the ring, there is one structure that represents separation of charges at A (negative charge) and D (positive charge). It is called a quinoid-like or through resonance structure (VIII). Such a situation cannot be realized for *meta*-disubstituted systems. The quinoid-like structure with localization of charges at D and A for *meta*-derivatives cannot be realized for canonical forms with single charge separation (Scheme 2).

To enable π-electron transfer from D to A in *meta*-derivative, the canonical forms with double charge separation have to be considered, as shown in Scheme 3.

Due to the lack of through resonance at the level of canonical forms with single charge separation for *meta*-disubstituted species, the resonance interactions associated with the π-electron structure are much less

**Correspondence to:* T. M. Krygowski, Department of Chemistry, Warsaw University, Pasteura 1, 02-093 Warsaw, Poland.
E-mail: tmkryg@chem.uw.edu.pl

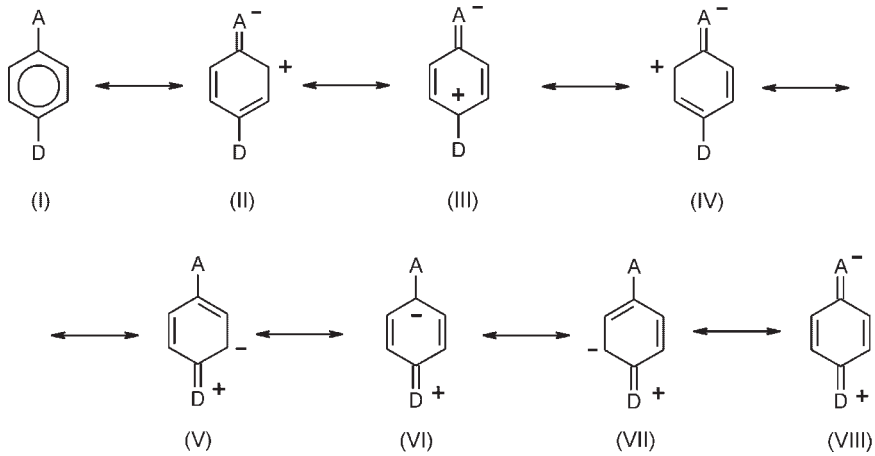

Scheme 1. Canonical forms with charge separation showing resonance effect between π-electron donating (D) and π-electron accepting (A) substituents in *para*-disubstituted benzene derivative

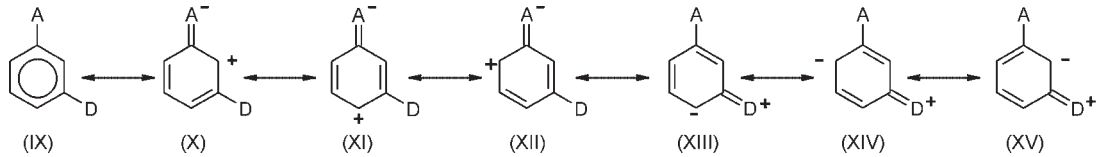

Scheme 2. Canonical forms with charge separation showing no resonance effect between π-electron donating (D) and π-electron accepting (A) substituents in *meta*-disubstituted benzene derivative

favorable than in the case of *para*-systems. In the case of *para* substitution, the D and A substituents exhibit different requirements for π-charges at the carbon atoms of the aromatic moiety. Those charges are distributed in a consisted way. In contrast, for *meta* substitution, this distribution is disconcerted and the charge demands are in conflict.[9] This is also nicely shown by the energy of homodesmotic reaction, presented in Scheme 4, suggested by Taft *et al*.[10] and measuring the stabilization of the system due to interactions between the substituents (Substituent Effect Stabilization Energy hereafter abbreviated as SESE).

SESE estimates the stabilization related to interactions through the π-electron ring between the π-electron donating substituent, D, and the π-electron accepting one, A. The SESE values computed for disubstituted benzene derivatives are usually greater for *para*-systems than for *meta*- ones. Simple STO-3G calculations of SESE for *p*- and *m*-nitrophenolate yield 30.4 and 17.6 kcal mole^{-1}, respectively.[11]

In the case of disubstituted naphthalene derivatives, the situation is much more complex. Many attempts have been made to study the substituent effects in naphthalene derivatives,[12] even applying the Hammett-like approaches,[13] but no general conclusion has been drawn so far. The number of possible, topologically different disubstituted naphthalene derivatives, even if we exclude *peri*- and *ortho*-substitution, is five times greater than that for benzene. Among them, there are five derivatives resembling *para*-substitution in benzene and five resembling the *meta*- one. The *para*-type interactions indicated in Scheme 5 may be described by quinoid canonical structure with localization of separated charges at A (negative charge) and D (positive charge) illustrated by canonical forms with charge separation. In the case of *meta*-type interactions, localization of separated charges at substituents requires canonical forms with double charge separation as shown in Scheme 6. Thus, we have to

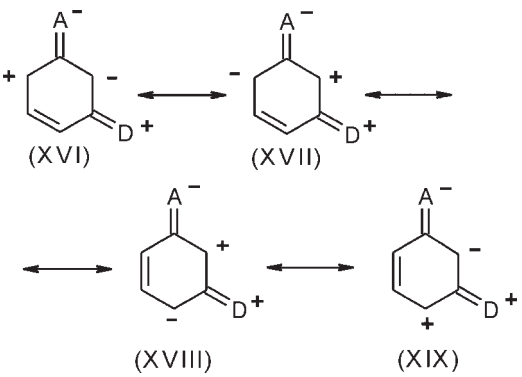

Scheme 3. Some of the canonical forms with double charge separation showing resonance effect between π-electron donating (D) and π-electron accepting (A) substituents in *meta*-disubstituted benzene derivative

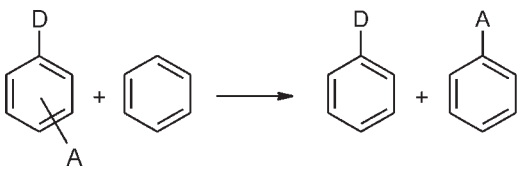

Scheme 4. Scheme of the homodesmotic reaction for calculation of Substituent Effect Stabilization Energy (SESE)

DOI: 10.1002/poc

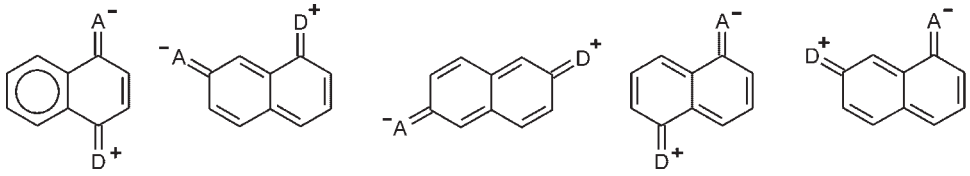

Scheme 5. Canonical forms with charge separation showing intramolecular charge transfer from π-electron donating (D) to π-electron accepting (A) group for *para*-type disubstituted naphthalenes

apply canonical forms with double charge separation to express an intramolecular charge transfer from D to A.

Moreover, each of the canonical forms with double charge separation from Scheme 6 should be represented by other excited structures with various localizations of charges at carbon atoms.

To analyze the problem of interaction between the π-electron donating, D, and π-electron accepting, A, substituents through the naphthalene moiety, we have chosen the —NO_2 group as A and —O^- as D. Thus, we were able to study how different topological situations for *para*- and *meta*-type disubstituted naphthalene derivatives differentiate the CN and CO bond lengths and their Atom in Molecules (AIM) characteristics as well as aromaticity of the rings and the whole naphthalene moiety.

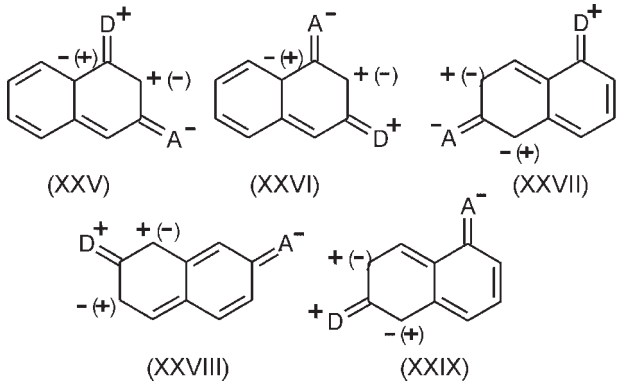

Scheme 6. Some of the canonical forms with double charge separation showing intramolecular charge transfer from π-electron donating (D) to π-electron accepting (A) group for *meta*-type disubstituted naphthalenes

METHODOLOGY

Molecular geometries of 10 isomers of nitronaphtholate shown in Scheme 7, 1- and 2-naphtholates, 1- and 2-nitronaphthalenes, *meta*- and *para*-nitrophenolates, phenolate, and nitrobenzene were optimized using Density Functional Theory at B3LYP/6-311G** level of approximation. The frequency analysis has been used to verify whether or not the optimized geometries correspond to the stationary points. The wave functions have been calculated for optimized systems at the same level of theory. All calculations were done using Gaussian 98.[14]

Scheme 7 presents various isomers of nitronaphthanolate together with labeling: **a** means that the —O^- substituent is in position 1 – (previously α-position), whereas **b** relates to position 2 – (previously β). The number following **a** and **b** indicates localization of the —NO_2 group.

The substituent effect on stability and π-electron delocalization in naphthalene moiety and the effect of mutual interactions between nitro- and —O^- substituents via the naphthalene moiety were studied by the use of homodesmotic reaction (Scheme 8) leading to SESE.

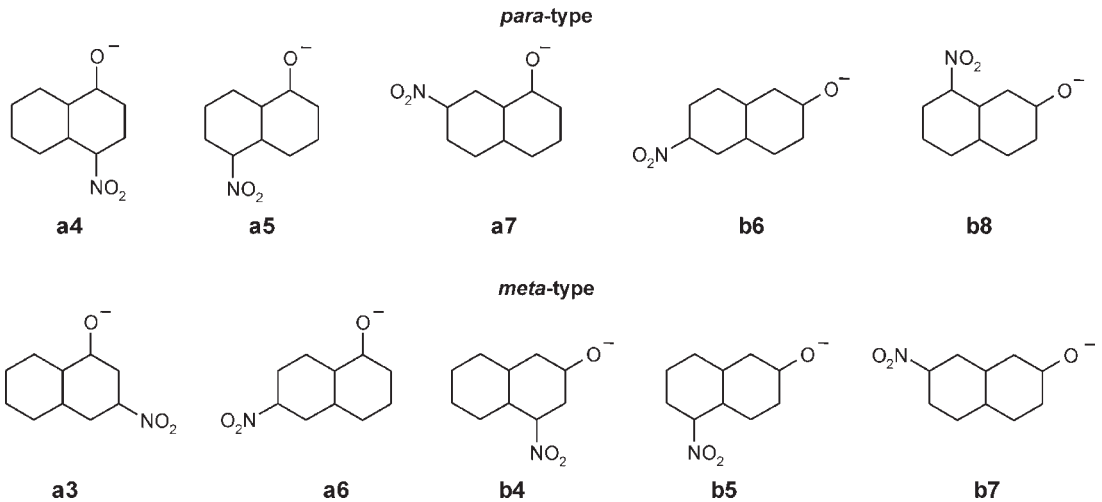

Scheme 7. Structures of studied nitronaphtholate isomers

DOI: 10.1002/poc

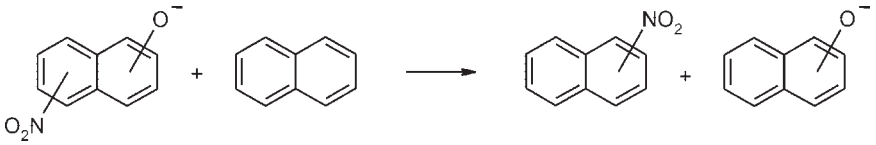

Scheme 8. Homodesmotic reaction for calculation of Substituent Effect Stabilization Energy (SESE) for nitronaphtholates

The changes in π-electron delocalization in particular rings were estimated by magnetism-based aromaticity indices Nucleus Independent Chemical Shift (NICS),[15] NICS(1),[16] and NICS(1)$_{zz}$[17] as well as by geometry-based index Harmonic Oscillator Model of Aromaticity (HOMA)[18] which was applied not only for individual rings, but also for the whole naphthalene moiety.

NICS[15] is the negative value of the absolute shielding estimated in the geometrical center of the ring, 1 Å above, NICS(1),[16] and its perpendicular to the ring component,[17] NICS(1)$_{zz}$. The NICSs values were calculated at HF/6-31 + G* using GIAO method as recommended by Schleyer *et al*.[15] The more negative the value of NICS is, the more aromatic is the system.[19]

Geometry-based index of aromaticity HOMA[18] is defined as in Eqn 1:

$$\mathrm{HOMA} = 1 - \frac{\alpha}{n}\sum_{i=1}^{n}(R_{\mathrm{opt}} - R_i)^2 \qquad (1)$$

where n is the number of bonds taken into the summation; α is a normalization constant (for CC bonds $\alpha = 257.7$) fixed to give HOMA = 0 for a model non-aromatic system (e.g., Kekulé structure of benzene for carbocyclic systems), and HOMA = 1 for the system with all bonds equal to the optimal value R_{opt} assumed to be realized for full aromatic systems (for CC bonds, R_{opt} is equal to 1.388 Å).

Topological analysis of electron density, ρ, has been performed on the basis of 'Atoms in Molecules' quantum theory proposed by Bader.[20] The AIM2000 package[21] was employed for determination and characterization of Bond Critical Points (BCP) by means of electron density, ρ, and its laplacian, $\nabla^2\rho$. Moreover, we have analyzed ellipticity and the ion/cov parameter based on the curvatures of electron density function around the BCP. Ellipticity is defined as $\varepsilon = (\lambda_1/\lambda_2) - 1$, where λ_1 and λ_2 correspond to two eigenvectors perpendicular to the direction of the bond (by definition: $\lambda_1 \leq \lambda_2 < 0$). This parameter illustrates how the electron density shape is flattened crosswise the bond path in BCP. The ε equals zero for ideally cylindrical bonds, for example, single or triple CC bond, and differs from zero when the bond cross-section is elliptic (see Table 1 for some examples of electron density, ρ, its laplacian, $\nabla^2\rho$, as well as ellipticity, ε, and ion/cov parameter). The ion/cov parameter is defined as $|\lambda_1|/\lambda_3$ ratio, where λ_1 is an eigenvalue (negative by definition) corresponding to eigenvector, which indicates the maximal decrease of electron density in the direction perpendicular to the direction of the bond and λ_3 is the eigenvalue (positive by definition) corresponding to eigenvector running along the direction of the bond.[22] Generally, the value of ion/cov parameter is <1 for bonds with partial closed-shell character, for example, ionic interactions, and >1 for interactions having mainly the covalent character.

RESULTS AND DISCUSSION

In order to analyze the complex situation in naphthalene derivatives, we start our discussion with the data for benzene derivatives. It is well known that *meta*- and *para*-disubstituted benzene derivatives differ significantly in terms of intramolecular interactions (substituent

Table 1. Bond lengths (d/Å) and selected AIM parameters of BCP's (electron density (ρ/ea$_0^{-3}$), its laplacian ($\nabla^2\rho$/ea$_0^{-5}$), eigenvectors, ellipticity (ε), and ion/cov parameter) for simple organic molecules

Molecule	Bond	d	ρ	$\nabla^2\rho$	λ_1	λ_2	λ_3	ε	ion/cov
Nitromethane	CN	1.530	0.242	−0.582	−0.471	−0.441	0.330	0.069	1.428
Ethane	CC	1.327	0.238	−0.532	−0.440	−0.440	0.349	0.000	1.261
Ethene	CC	1.337	0.345	−1.033	−0.747	−0.559	0.273	0.338	2.740
Butadiene	CC double	1.456	0.340	−1.009	−0.736	−0.556	0.282	0.323	2.606
	CC single	1.421	0.277	−0.726	−0.560	−0.514	0.348	0.089	1.608
Methanol	CO	1.305	0.256	−0.504	−0.472	−0.468	0.435	0.008	1.084
Methanolate anion	CO	1.127	0.343	−0.780	−0.741	−0.741	0.701	0.000	1.056
Carbon oxide	CO	1.200	0.489	0.647	−1.634	−1.634	3.914	0.000	0.417
Formic aldehyde	CO	1.467	0.416	0.085	−1.088	−1.037	2.210	0.049	0.492
Methylamine	CN	1.266	0.261	−0.670	−0.516	−0.498	0.344	0.037	1.501
Methylimine	CN	1.503	0.389	−0.897	−0.908	−0.753	0.765	0.206	1.188
Nitromethane	CN	1.503	0.242	−0.582	−0.471	−0.441	0.330	0.069	1.428
Carbon dioxide	CO	1.185	0.435	−0.215	−1.078	−1.078	1.941	0.000	0.555
Beryllium oxide	BeO	1.321	0.173	1.779	−0.418	−0.418	2.614	0.000	0.160

DOI: 10.1002/poc

Table 2. Total electron energy (*E*/hartree), substituent effect stabilization energy (SESE/kcal mole^{-1}), bond lengths (*d*/Å), HOMA, and NICSs values for benzene, phenolate, nitrobenzene, *meta*- and *para*-nitrophenolate

Molecule	HOMA	*E*	SESE	*d*(CO)	*d*(CN)	NICS	NICS(1)	NICS(1)$_{zz}$
Benzene	0.99	−232.2084	—	—	—	−9.72	−11.54	−31.90
Phenolate	0.66	−306.8859	—	1.262	—	−6.09	−7.46	−21.31
Nitrobenzene	0.99	−436.7619	—	—	1.480	−10.92	−11.67	−30.48
m-Nitrophenolate	0.66	−511.4644	15.69	1.255	1.475	−7.83	−8.01	−20.95
p-Nitrophenolate	0.49	−511.4810	26.10	1.248	1.416	−3.80	−5.64	−12.00

effect). This is well illustrated by, for example, SESE values for *meta*- and *para*-nitrophenolate, which are 15.69 and 26.10 kcal mole^{-1}, respectively (Table 2).

Analysis of *meta*- and *para*-nitrophenolates

Table 2 contains the data describing energetics (SESE and total electron energies) as well as HOMA and NICSs values for benzene, nitrobenzene, phenolate, *meta*- and *para*-nitrophenolates.

It results from the data in Table 2 that *para*-nitrophenolate anion is more stable than its *meta*-isomer by 10.4 kcal mole^{-1}, and obviously, the same is the difference between SESE values for these compounds. However, HOMA and NICSs values show that the ring in the *para*-isomer is less aromatic than in the *meta*- one. This means that an increase of stability of the molecule as a whole is associated with a decrease of cyclic π-electron delocalization. The increase of through resonance interaction due to the substituent effect acts against cyclic π-electron delocalization being mostly attributed to the notion of aromaticity.[23] Interestingly, the difference shown by NICS indices is the greatest for NICS(1)$_{zz}$.

Table 3 presents CN and CO bond lengths as well as the electron density, ρ, its laplacian, $\bigtriangledown^2\rho$, ellipticity, ε, and ion/cov parameter in their BCP. Because of stronger interactions between substituents in *para*-isomer than in the *meta*- one, the CN and CO bond lengths in *para*-isomer are shorter than in *meta*- one. The difference for CN bond length (0.059 Å) is significantly greater than that for CO (0.007 Å). Similar differences for CN bond in these two isomers are also found for ellipticities (0.185) and ion/cov parameter (0.111). These differences for CO bond are smaller, 0.006 for ellipticities and 0.049 for ion/cov parameter. For the *m*-nitrophenolate, ε of CN bond is close to that for nitrobenzene indicating the lack of through resonance effect. Ellipticity of CN is significantly greater in the *para*-isomer than in the *meta*- one, but simultaneously the bond loses some covalency as shown by the ion/cov parameter. Ellipticity of CO bond in both *para*- and *meta*-nitrophenolates is low, around 0.03–0.04, and resembles rather the value for formic aldehyde ($\varepsilon = 0.049$, Table 1) than for methanolate anion ($\varepsilon = 0.000$). The values of ion/cov parameter for *m*- and *p*-nitrophenolate are 0.682 and 0.633, respectively, and are little different from the value for formic aldehyde (0.492), but dramatically lower than that for methanolate (1.056). This indicates a highly polarized CO bond, oppositely to that of CN, which is more covalent in nature, with the values of 1.460 and 1.571, for *para*- and *meta*-isomers, respectively. Thus, a strong through resonance effect in *para*-isomer causes a significantly more polarized covalent bond than in the *meta*- one.

It is known from the studies on aromaticity of the ring in monosubstituted benzene derivatives[24] that substituents with a lone pair accessible for resonance with the ring (e.g., —O$^-$) affect strongly cyclic π-electron delocalization. This is not the case for —NO$_2$ group, which practically does not affect aromaticity of the ring (Table 2). In the case of disubstituted benzene derivatives, there is practically no change in delocalization for *m*-nitrophenolate as compared with phenolate, and a substantial decrease for *p*-nitrophenolate.

Analysis of nitro-derivatives of 1- and 2-naphtholates

The intramolecular interaction between the —O$^-$ and —NO$_2$ substituents in the nitronaphtholates derivatives may be analyzed from three points of view: (i) an increase

Table 3. Electron density (ρ/ea$_0^{-3}$), its laplacian ($\bigtriangledown^2\rho$/ea$_0^{-5}$), ellipticity, and ion/cov parameter in the CO and CN bond critical points along with its bond lengths (*d*/Å) for phenolate, nitrobenzene, *para*- and *meta*-nitrophenolate

	CN bond					CO bond				
Molecule	ρ	$\bigtriangledown^2\rho$	ε	ion/cov	*d*	ρ	$\bigtriangledown^2\rho$	ε	ion/cov	*d*
Phenolate	—	—	—	—	—	0.369	−0.461	0.029	0.693	1.262
Nitrobenzene	0.256	−0.660	0.122	1.594	1.480	—	—	—	—	—
m-Nitrophenolate	0.250	−0.600	0.130	1.571	1.475	0.375	−0.445	0.039	0.682	1.248
p-Nitrophenolate	0.280	−0.608	0.315	1.460	1.416	0.379	−0.355	0.033	0.633	1.255

DOI: 10.1002/poc

Table 4. Electron density (ρ/ea$_0^{-3}$), its laplacian ($\nabla^2\rho$/ea$_0^{-5}$), ellipticity (ε), and ion/cov parameter calculated in CN and CO bond critical points and corresponding bond lengths (d/Å) for monosubstituted naphthalene derivatives and all 10 nitronaphtholates (for labeling, see Scheme 7)

	CN bond					CO bond				
Molecule	ρ	$\nabla^2\rho$	ε	ion/cov	d	ρ	$\nabla^2\rho$	ε	ion/cov	d
					Meta-type					
a3	0.248	−0.602	0.111	1.562	1.482	0.376	−0.397	0.037	0.656	1.252
a6	0.258	−0.634	0.151	1.633	1.463	0.375	−0.398	0.033	0.656	1.253
b4	0.252	−0.614	0.139	1.598	1.475	0.376	−0.437	0.042	0.678	1.253
b5	0.253	−0.622	0.135	1.613	1.474	0.375	−0.412	0.034	0.663	1.254
b7	0.257	−0.633	0.153	1.632	1.464	0.376	−0.412	0.037	0.663	1.253
					Para-type					
a4	0.277	−0.606	0.354	1.519	1.420	0.381	−0.306	0.027	0.608	1.244
a5	0.264	−0.643	0.222	1.675	1.450	0.377	−0.355	0.030	0.633	1.250
a7	0.270	−0.656	0.221	1.648	1.440	0.380	−0.347	0.034	0.630	1.247
b6	0.275	−0.652	0.253	1.605	1.429	0.379	−0.361	0.036	0.636	1.249
b8	0.267	−0.650	0.240	1.688	1.445	0.378	−0.354	0.035	0.633	1.249
					Monosubstituted naphthalene derivatives					
1-Nitronaphthalene	0.255	−0.652	0.128	1.595	1.481	—	—	—	—	—
1-Naphtholate	—	—	—	—	—	0.372	−0.407	0.029	0.662	1.257
2-Nitronaphthalene	0.257	−0.664	0.127	1.610	1.478	—	—	—	—	—
2-Naphtholate	—	—	—	—	—	0.372	−0.430	0.033	0.674	1.257

of quinoid structure weight should lead to a shortening of CO and CN bonds; (ii) an increase of quinoid structure weight should lead to an increase of stabilization characterized by SESE values; (iii) an increase of quinoid structure is associated with a decrease of cyclic π-electron delocalization which may be measured by aromaticity indices (e.g., NICS, HOMA).

Interrelation between bond lengths and AIM parameters. It is well known that in many cases, AIM parameters in BCP correlate with bond length.[25] Table 4 presents AIM parameters for all 10 nitronaphtholates as well as for monosubstituted naphthalene derivatives with —O$^-$ or —NO$_2$ as substituent.

When electron density in BCP of CO and CN bonds are plotted against their lengths, the regressions are linear as shown in Figs. 1 and 2.

In both cases, elongation of the bond is associated with a decrease of charge density in BCP. This is in line with an observation found for CC bonds in benzenoid hydrocarbons.[25c,26] Interestingly, the *para*- and *meta*-type of naphthalene derivatives form two separated parts of the scatter plots in Figs. 1 and 2. In both cases, the *para*-isomers have shorter CN and CO bonds and higher electron density in BCP than *meta*-isomers. This proves

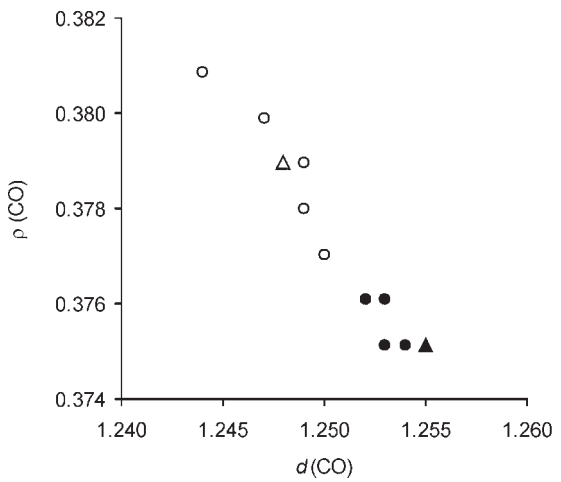

Figure 1. Dependence of ρ(CO) on d(CO) for nitronaphtholates. Correlation coefficient $cc = -0.974$. Open circles stand for *para*-type and filled circles for *meta*-type. The open and filled triangles stand for *p*-nitrophenolate and *m*-nitrophenolate, respectively

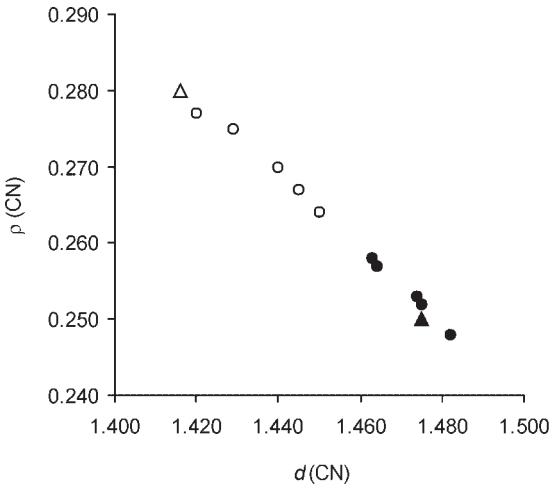

Figure 2. Dependence of ρ(CN) on d(CN) for nitronaphtholates. Correlation coefficient $cc = -0.997$. Open circles s tand for *para*-type and filled circles for *meta*-type. The open and filled triangles stand for *p*-nitrophenolate and *m*-nitrophenolate, respectively

DOI: 10.1002/poc

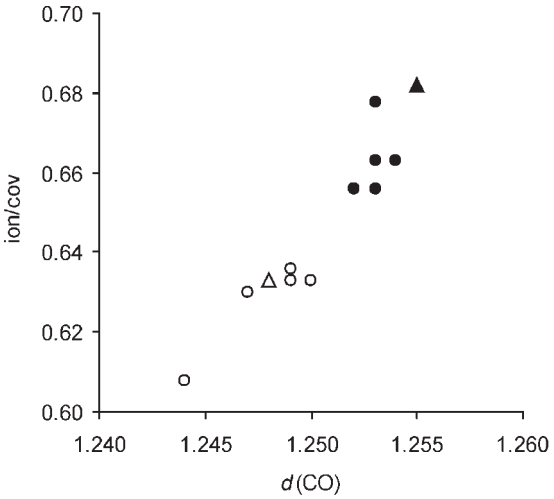

Figure 3. Dependence of ion/cov(CO) on *d*(CO) for nitronaphtholates. Correlation coefficient $cc = 0.949$. Open circles stand for *para*-type and filled circles for *meta*-type. The open and filled triangles stand for *p*-nitrophenolate and *m*-nitrophenolate, respectively

that in *para*-type derivatives, the substituent effect is stronger than in *meta*-type ones. Moreover, when we add to both plots the points for *para*- and *meta*-nitrophenolates, these points fit well the groups for *para*- and *meta*-type naphthalene derivatives.

Figures 3 and 4 show how the polarity of the bond expressed by ion/cov parameter for *para*- and *meta*-type derivatives depends on CO and CN bond lengths. In the first case, we see a roughly linear dependence of ion/cov(CO) on *d*(CO). The longer the bond is, the higher contribution of covalency is observed. For *meta*-type derivatives, the CO bond exhibits a more covalent character than for *para*-isomers. In both cases, the data for

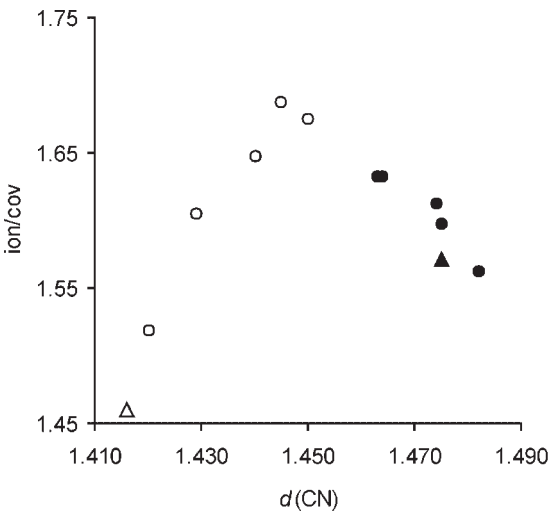

Figure 4. Dependence of ion/cov(CN) on *d*(CN) for nitronaphtholates. Open circles stand for *para*-type and filled circles for *meta*-type. The open and filled triangles stand for *p*-nitrophenolate and *m*-nitrophenolate, respectively

meta- and *para*-nitrophenolate fit well the appropriate group of naphthalene derivatives.

A dramatic difference is observed for the dependence of ion/cov(CN) on *d*(CN). In this case, for the *para*-type naphthalene derivatives, the regression has a positive slope with $cc = 0.961$, whereas the slope for the *meta*-type isomers is negative, $cc = -0.908$. Again, the points for *para*- and *meta*-nitrophenolate fit well the appropriate group of naphthalene derivatives.

The observed dependence may be interpreted as follows. It is well known that the substituent effect is composed of two factors:[1c,5,7,8] a field (inductive) factor and a resonance (mesomeric) factor, both of which affect the geometry of the molecule. However, there is still another factor affecting significantly the molecular structure – this is electronegativity of the substituent.[27] The resonance effect depends strongly on cooperative interactions between two substituents. In disubstituted π-electron systems, the resonance effect dominates only for substituents of strong and opposite resonance power, whereas the electronegativity effect is local and depends only on the kind of substituent. The substituent of much different electronegativity than the substituted carbon atom affects dramatically its hybridization, which may be described by the Bent–Walsh rule[27a,28] and results in changes of *ipso*-bond angle and *ipso-ortho* CC bond lengths.[29] Moreover, it is known from basic chemistry that the greater is the difference in electronegativity of two atoms forming the bond, the greater is its polarity.[30]

In the case of *para*-type isomers, the through resonance effect leading to a quinoid-like structure is the strongest of the three factors mentioned above. The greater the weight of quinoid canonical structure is, the shorter the CN bond becomes and more the charge is localized on $—NO_2$ group. This effect increases the polarity of CN bond.[31] The most effective through resonance and in consequence, a high contribution of quinoid-like structure is for *p*-nitrophenolate, since there is only one π-electron ring and there is no other possibility for charge dispersion on another ring, as it is in the case of naphthalene derivatives. The quinoid-like structure in *para*-type naphthalene derivatives may be formed involving one or two rings. The first case is realized only for one isomer – **a4**. Only in this case, the Clar sextet[32] may be drawn and explain the increase of stability of this particular system. Here, an increase of stability is due to two different and, in many other cases, opposite factors. In the case of **a4**, these factors cooperate. The disubstituted ring is strongly stabilized, whereas the side ring increases global stabilization due to its cyclic delocalization. In all other cases of *para*-type nitronaphtholates, both rings are involved in intramolecular charge transfer leading to weaker charge transfer from $—O^-$ to $—NO_2$ and more dispersed charge over two rings. It is worth mentioning that the nitro- group as a substituent has a large field/inductive effect ($F = 0.65$)[33] and an equally strong resonance effect ($R = 0.62$), so total interaction with the

DOI: 10.1002/poc

π-electron donating system is characterized by $\sigma^- = 1.27$. Thus, in the case of *para*-type intramolecular interactions, the resonance effect seems to be dominant.

The situation for *meta*-type isomers is quite different because the resonance effect is definitely weaker since it needs canonical forms with double charge separation to be considered (Scheme 6). Therefore, the dominant effect is related to the inductive and electronegativity effects of —NO_2 group. The electronegativity of —NO_2 group is high – in the Pauling scale,[34] it is equal to 4.19[35] or 4.33[36] which may be decisive for the changes of the ion/cov parameter. The longer the bond is, the more charge is attracted by the electronegative nitro- group and in consequence, the more polarized the CN bond is.

Another possible interpretation is that elongation of the CN bond results in a decrease of its strength. This is documented by a dependence of electron density at BCP on bond length (Fig. 1) An increase of interatomic distance affects much more weakly electrostatic contribution to the interaction than the covalent one. As a result, the ionic character of the bond increases.

Interrelations between SESE, HOMA, and NICSs. Interactions between —O^- and —NO_2 substituents also affect non-local parameters describing energetics and π-electron delocalization of the molecule. The SESE values (Table 5) characterizing the 'strength' of interactions between both substituents through the naphthalene moiety, may be divided into two groups: the data for *para*-type systems and for *meta*-type ones. The *para*-systems have a much higher mean value of SESE (17.42 kcal mole^{-1}) and the lowest SESE value for this set of data (**b8**) equals 14.06, being higher than the highest SESE value for *meta*-type systems (12.80 kcal mole^{-1} for **a3**). The mean SESE for *meta*-systems is 11.90 kcal mole^{-1}. Definitely, the stabilization due to substituent effects in *para*-systems is greater than in *meta*- ones. Another important difference between SESE values for the *para*- and *meta*-systems is in the range of SESE values. For *meta*-type, it is only 2.32 kcal mole^{-1}, whereas for *para*-type it is 10.22 kcal mole^{-1}. This may suggest that topological differences in localization of substituents for *meta*-systems practically do not differentiate SESE values.

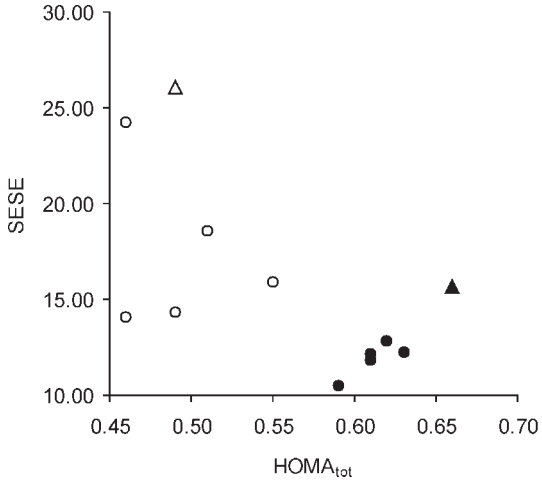

Figure 5. Dependence of SESE on HOMA$_{tot}$ for nitronaphtholates. Open circles stand for *para*-type and filled circles for *meta*-type. The open and filled triangles stand for *p*-nitrophenolate and *m*-nitrophenolate, respectively

Table 5. HOMA, total energy (E_{total}/hartree), relative total energy (E_{rel}/kcal mole^{-1}), substituent effect stabilization energy (SESE/kcal mole^{-1}), CO and CN bond lengths (d(CO), d(CN)/Å) for 10 nitronaphtholates (for labeling, see Scheme 7), nitronaphthalenes, and naphtholates

	HOMA			*E*				
Molecule	Ring 1	Ring 2	tot	total	rel	SESE	d(CO)	d(CN)
				Meta-type				
a3	0.41	0.81	0.62	−665.1051	7.15	12.80	1.252	1.482
a6	0.34	0.81	0.63	−665.1042	7.72	12.24	1.253	1.463
b4	0.43	0.70	0.61	−665.0936	14.37	11.80	1.253	1.475
b5	0.37	0.67	0.59	−665.0915	15.69	10.48	1.254	1.474
b7	0.39	0.73	0.61	−665.1011	9.66	12.17	1.253	1.464
				Para-type				
a4	0.08	0.85	0.46	−665.1165	0.00	24.28	1.244	1.420
a5	0.22	0.64	0.49	−665.1006	9.98	14.31	1.250	1.450
a7	0.30	0.73	0.54	−665.1100	4.08	15.88	1.247	1.440
b6	0.28	0.64	0.51	−665.1113	3.26	18.57	1.249	1.429
b8	0.21	0.54	0.46	−665.0972	12.11	14.06	1.249	1.445
				Monosubstituted naphthalene derivatives				
1-Nitronaphthalene	0.75	0.76	0.79	−590.3854	4.33	—	—	1.488
1-Naphtholate	0.39	0.80	0.61	−460.5304	0.00	—	1.257	—
2-Nitronaphthalene	0.79	0.79	0.82	−590.3923	0.00	—	—	1.478
2-Naphtholate	0.40	0.71	0.59	−460.5274	1.88	—	1.257	—
Naphthalene	0.79	0.79	0.81	−385.8380	—	—	—	—

DOI: 10.1002/poc

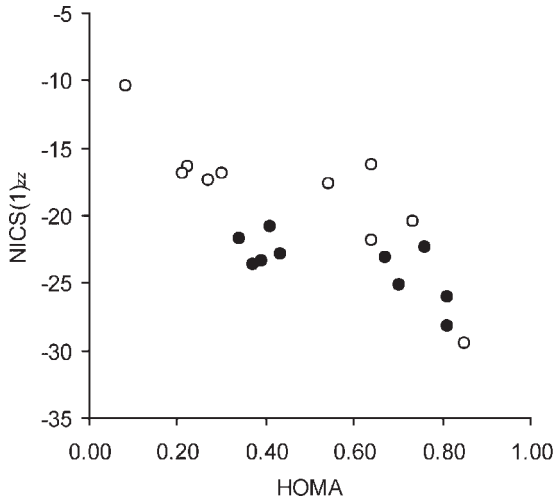

Figure 6. Dependence of NICS(1)$_{zz}$ on HOMA for each ring in nitronaphtholates. Open circles stand for *para*-type and filled circles for *meta*-type

Obviously, the same results are observed for the values of total electron energies, *E*.

A similar observation is found for HOMA values calculated for the whole aromatic moiety, HOMA$_{tot}$. For *para*-type molecules the mean value of HOMA$_{tot}$ is 0.49, whereas for *meta*-type, it is 0.61. Thus, again, as in other cases,[23,37] cyclic π-electron delocalization described here by HOMA$_{tot}$ is lowered by through resonance interactions between —NO_2 and —O^-, especially for *para*-type systems. Interestingly, the above-discussed quantities, SESE *versus* HOMA$_{tot}$, are separated into two clusters for *meta*- and *para*-types, as shown in Fig. 5.

Analysis of HOMA values calculated for individual rings leads to a similar picture. In both kinds of rings, the mean values of HOMA are lower for *para*-type systems (0.22 and 0.68, respectively) than for *meta*-type systems (0.39 and 0.75, respectively). HOMA for individual rings may be compared with NICSs appropriate only for local aromatic properties. Figure 6 presents the dependencies of NICS(1)$_{zz}$ (Table 6) on HOMA values for rings 1 and 2. The ring is labeled as 1 if substituted with —O^-.

Data for rings 1 present an approximate linear dependence with lower aromaticity (higher NICS(1)$_{zz}$ and lower HOMA values) for *para*-type systems and higher for *meta*-type systems. This kind of separation of *meta*- and *para*-systems is not observed for the dependence of NICS(1)$_{zz}$ on HOMA for ring 2. The difference between rings 1 and 2 consists in the presence of a direct influence of —O^- substituent on ring 1. Comparison of aromaticity indices for monosubstituted naphthalene derivatives: 1- or 2-nitronaphthalene and 1- or 2-naphtholate shows that the —O^- substituent affects the aromatic moiety much more strongly than the nitro-group. HOMA values for the whole moiety for naphtholates are around 0.40, whereas for nitro-derivatives are not much lower than for naphthalene itself (0.79). A similar picture can be seen for HOMA and NICSs values for individual rings. The —O^- substituent affects much more strongly π-electron delocalization in the naphthalene moiety than the nitro- group does. The same is true for individual rings, independently of the ring. This strong effect of the —O^- substituent is in line with an observation made for monosubstituted benzene derivatives[24] – the substituents with a lone pair or a vacant orbital of an appropriate symmetry affect strongly the π-electron structure of the ring.

Table 6. NICS, NICS(1), and NICS(1)$_{zz}$ values for each ring in 10 nitronaphtholates (for labeling, see Scheme 7), nitronaphthalenes, and naphtholates

	Ring 1			Ring 2		
Molecule	NICS	NICS(1)	NICS(1)$_{zz}$	NICS	NICS(1)	NICS(1)$_{zz}$
			Meta-type			
a3	−7.75	−8.25	−20.70	−8.83	−10.50	−28.13
a6	−6.00	−8.05	−21.66	−9.98	−10.40	−26.03
b4	−8.90	−9.31	−22.86	−7.90	−9.36	−25.07
b5	−7.08	−8.97	−23.50	−9.03	−9.21	−23.05
b7	−6.91	−8.97	−23.36	−8.72	−9.09	−22.32
			Para-type			
a4	−2.55	−4.88	−10.34	−9.54	−10.99	−29.41
a5	−3.60	−6.16	−16.27	−8.21	−9.07	−21.83
a7	−3.86	−6.39	−16.85	−7.74	−8.69	−20.34
b6	−4.26	−6.97	−17.32	−6.18	−7.27	−16.14
b8	−3.93	−6.79	−16.78	−6.80	−7.52	−17.56
			Monosubstituted naphthalene derivatives			
1-Nitronaphthalene	−10.99	−11.57	−29.34	−10.04	−11.81	−31.58
1-Naphtholate	−5.66	−7.57	−20.55	−8.83	−10.32	−27.91
2-Nitronaphthalene	−11.01	−11.64	−29.32	−9.70	−11.66	−31.03
2-Naphtholate	−6.76	−8.61	−22.58	−7.48	−8.92	−23.94
Naphthalene	−9.90	−11.64	−31.26	−9.89	−11.63	−31.25

DOI: 10.1002/poc

CONCLUSIONS

All observables have a common characteristic feature, namely that the *para*- and *meta*-type derivatives form clusters to which the mother compounds *p*- and *m*-nitrophenolates, respectively, fit well. —O^- is the dominant substituent, however another one, —NO_2 undergoes stronger changes in both structural and electronic ways. *Para*-type systems usually exhibit a stronger variation in any kind of parameters than the *meta*-type ones.

Acknowledgements

We thank the Interdisciplinary Center for Mathematical and Computational Modeling (Warsaw, Poland) for computational facilities. M.P. wishes to thank the Rector of the University of Łódź for financial support (University Research Grants – grant No. 505/706 2006). TMK kindly acknowledges financial support from MNII grant No. 3 T09A 031 28.

REFERENCES

1. (a)Hammett LP. *Physical Organic Chemistry*, McGraw-Hill: New York, 1st ed. 1940 and 2nd ed. 1970.(b)Jaffe HH, *Chem. Rev.* 1953; **53**: 191–261.(c)Charton M. *Progr. Phys. Org. Chem.* 1981; **13**: 119–251.(d)Exner O. In *Correlation Analysis of Chemical Data*, Chapman NB, Shorter J (eds). Plenum Press: New York, 1988; Chapter 10, 439ff.(e)Palm VA. *Osnovy kolichestvennnoy teoryi organitcheskikh soedineni*. Izd. Khimya: Leningrad, 1967.(f)Chapman NB, Shorter J (eds). *Correlation Analysis in Chemistry – Recent Advances*, Plenum Press: London, 1978; 119–173 and 439–540.
2. Hammett LP. *Physical Organic Chemistry*, 1st ed. McGraw-Hill: NewYork, 1940; 196.
3. Hammett LP. *Physical Organic Chemistry*, 1st ed. McGraw-Hill: New York, 1940; 184.
4. Brown HC, Okamoto Y. *J. Am. Chem. Soc.* 1958; **80**: 4979–4987.
5. Shorter J. In *Similarity Models in Organic Chemistry, Biochemistry and Related Fields*, Zalewski RI, Krygowski TM, Shorter J (eds). Elsevier: Amsterdam, 1991; Chapter 2, 77f.
6. Taft RW. *J. Phys. Chem.* 1960; **64**: 1805–1815.
7. Exner O. *Collect. Czech. Chem. Comm.* 1966; **31**: 65–89.
8. Taft RW, Lewis IC. *J. Am. Chem. Soc.* 1958; **80**: 2436–2443.
9. Eckert-Maksić M, Klessinger M, Maksić ZB. *J. Phys. Org. Chem.* 1995; **8**: 435–441.
10. Pross A, Radom L, Taft WR. *J. Org. Chem.* 1980; **45**: 818–826.
11. Hehre WJ, Radom L, Schleyer PvR, Pople JA. *Ab initio Molecular Orbital Theory.* Wiley: New York, 1986; 361.
12. (a)Dewar MJS, Grisdale P. *J. Am. Chem. Soc.* 1962; **84**: 3546–3548.(b)Wells PR, Adcock W. *Aust. J. Chem.* 1965; **18**: 1365–1376.(c)Adcock W, Dewar MJS. *J. Am. Chem. Soc.* 1967; **89**: 379–385.(d)Kovaček D, Maksić ZB, Novak I. *J. Phys. Chem. A* 1997; **101**: 1147–1154.(e)Eckert-Maksić M, Klessinger M, Antol I, Maksić ZB. *J. Phys. Org. Chem.* 1997; **10**: 415–419.
13. (a)Dewar MJS, Grisdale P. *J. Am. Chem. Soc.* 1962; **84**: 3539–3541.(b)Dewar MJS, Grisdale P. *J. Am. Chem. Soc.* 1962; **84**: 3548–3553.(c)Pytela O. *Collect. Czech. Chem. Comm.* 1995; **60**: 1502–1528.
14. Frisch MJ, Trucks GW, Schlegel HB, Scuseria GE, Robb MA, Cheeseman JR, Zakrzewski VG, Montgomery JA Jr, Stratmann RE, Burant JC, Dapprich S, Millam JM, Daniels AD, Kudin KN, Strain MC, Farkas O, Tomasi J, Barone V, Cossi M, Cammi R, Mennucci B, Pomelli C, Adamo C, Clifford S, Ochterski J, Petersson GA, Ayala PY, Cui Q, Morokuma K, Malick DK, Rabuck AD, Raghavachari K, Foresman JB, Cioslowski J, Ortiz JV, Baboul AG, Stefanov BB, Liu G, Liashenko A, Piskorz P, Komaromi I, Gomperts R, Martin RL, Fox DJ, Keith T, Al-Laham MA, Peng CY, Nanayakkara A, Gonzalez C, Challacombe M, Gill PMW, Johnson B, Chen W, Wong MW, Andres JL, Gonzalez C, Head-Gordon M, Replogle ES, Pople JA. *Gaussian 98*, Revision A.7. Gaussian, Inc.: Pittsburgh, PA, 1998.
15. Schleyer PvR, Maerker C, Dransfeld A, Jiao H, Hommes NJRvE. *J. Am. Chem. Soc.* 1996; **118**: 6317–6318.
16. Schleyer PvR, Manoharan M, Wang Z-X, Kiran B, Jiao H, Puchta R, Hommes NJRvE. *Org. Lett.* 2001; **3**: 2465–2468.
17. Corminboeuf C, Heine T, Seifert G, Schleyer PvR, Weber J. *Phys. Chem. Chem. Phys.* 2004; **6**: 273–276.
18. Krygowski TM. *J. Chem. Inf. Comput. Sci.* 1993; **33**: 70–78.
19. Chen Z, Wannere CS, Corminboeuf C, Puchta R, Schleyer PvR . *Chem. Rev.* 2005; **105**: 3842–3888.
20. Bader RFW. *Atoms in Molecules: A Quantum Theory.* Oxford University Press: New York, 1990.
21. AIM2000 designed by Friedrich Biegler-König, University of Applied Sciences, Bielefeld, Germany.
22. (a)Solà M, Mestres J, Carbo R, Duran M. *J. Chem. Phys.* 1996; **104**: 636–647.(b)Bader RFW. *Atoms in Molecules, A Quantum Theory.* Oxford University Press: Oxford, 1990; Chapter 7.4, 288.
23. Krygowski TM, Stępień BT. *Chem. Rev* 2005; **105**: 3482–3512.
24. (a)Krygowski TM, Stępień BT. *Pol. J. Chem.* 2004; **78**: 2213–1227.(b)Krygowski TM, Ejsmont K, Stępień BT, Cyrański MK, Poater J, Solà M. *J. Org. Chem.* 2004; **69**: 6634–6640.
25. (a)O'Brien SE, Popelier PLA. *Can. J. Chem.* 1999; **77**: 28–36.(b)Mallinson PR, Smith GT, Wilson CC, Grech E, Woźniak K. *J. Am. Chem. Soc.* 2003; **125**: 4259–4270.(c)Howard ST, Krygowski TM. *Can. J. Chem.* 1997; **75**: 1174–1181.
26. Bader RFW, Tang TH, Tal Y, Biegler-Koenig FW. *J. Am. Chem. Soc.* 1982; **104**: 946–952.
27. (a)Domenicano A, Vaciago A, Coulson C. *Acta Cryst. B* 1975; **31**: 1630–1641.(b)Campanelli AR, Domenicano A, Ramondo F. *J. Phys. Chem. A* 2003; **107**: 6429–6440.
28. (a)Walsh AD. *Discuss. Faraday Soc.* 1947; **2**: 18–25.(b)Bent HA. *Chem. Rev.* 1961; **61**: 275–311.
29. Krygowski TM, Szatyłowicz H. *Pol. J. Chem.* 2004; **78**: 1719–1731.
30. Pauling L. *The Nature of the Chemical Bond*. Cornell University Press: Ithaca, 1960; 79.
31. Exner O, Krygowski TM. *Chem. Soc. Rev.* 1996; **25**: 71–75.
32. (a)Clar E. *Polycyclic Hydrocarbons*. Academic Press: London, 1964.(b)Clar E. *Aromatic Sextett*. Wiley: London, 1972.
33. Hansch C, Leo A, Taft RW. *Chem. Rev.* 1991; **91**: 165–195.
34. Pauling L. *The Nature of the Chemical Bond*. Cornell University Press: Ithaca, 1960; 88.
35. Campanelli AR, Domenicano A, Ramondo F, Hargittai I. *J. Phys. Chem. A* 2004; **108**: 4940–4948.
36. (a)Huheey JE. *J. Phys. Chem.* 1965; **69**: 3284–3291.(b)Huheey JE. *J. Phys. Chem.* 1966; **70**: 2086–2092.
37. Krygowski TM, Stępień BT, Cyrański MK, Ejsmont K. *J. Phys. Org. Chem.* 2005; **18**: 886–891.

DOI: 10.1002/poc